

Groundwater potentiality mapping of hard-rock terrain in arid regions using geospatial modelling: example from Wadi Feiran basin, South Sinai, Egypt

Mohamed O. Arnous¹

Received: 2 November 2015 / Accepted: 4 April 2016 / Published online: 25 April 2016
© Springer-Verlag Berlin Heidelberg 2016

Abstract Identifying a good site for groundwater exploitation in hard-rock terrains is a challenging task. In Sinai, Egypt, groundwater is the only source of water for local inhabitants. Interpretation of satellite data for delineation of lithological units and weathered zones, and for mapping of lineament density and their trends, provides a valuable aid for the location of groundwater promising areas. Complex deformational histories of the wide range of lithological formations add to the difficulty. Groundwater prospect mapping is a systematic approach that considers the major controlling factors which influence the aquifer and quality of groundwater. The presented study aims to delineate, identify, model and map groundwater potential zones in arid South Sinai using remote sensing data and a geographic information system (GIS) to prepare various hydromorphogeological thematic maps such as maps of slope, drainage density, lithology, landforms, structural lineaments, rainfall intensity and plan curvature. The controlling-factor thematic maps are each allocated a fixed score and weight, computed by using a linear equation approach. Furthermore, each weighted thematic map is statistically computed to yield a groundwater potential zone map of the study area. The groundwater potential zones thus obtained were divided into five categories (very poor, poor, moderate, good and very good) and were validated using the relation between the zone and the spatial distribution of productive wells and of previous geophysical investigations from a literature review. The results show the groundwater potential zones in the study area, and create awareness for better planning and management of groundwater resources.

Keywords Remote sensing · Geographic information systems · Groundwater exploration · Modelling · Egypt

Introduction

Groundwater is a vital natural resource for sustainable-development planning around the world, particularly for agricultural and industrial activities. In addition, the need to develop groundwater resources to the maximum possible extent has gained importance. There is a corresponding need to identify, delineate, map and assess the factors controlling groundwater accumulation, in order to predict and explore the probable exploitation sites, thus supporting effective groundwater planning and development. Arid regions suffer from severe water scarcity. Groundwater resources are crucially important in arid and semi-arid regions, since the rainfall and, subsequently, the surface-water availability are very unpredictable. Although the extractable amounts of groundwater are directly related to precipitation, the seasonal storage of groundwater is much higher than for surface water, and groundwater is often used as a back-up during the dry season or dry spells. Many arid and semi-arid areas are underlain by hard rocks in which the primary porosity and hydraulic conductivity are low and the groundwater resides mainly in fractures or weathered zones of the bedrock, generally referred to as secondary porosity and secondary hydraulic conductivity (Gustafsson 1994). From a groundwater exploration approach, the term ‘hard rock’ can comprise all rocks without sufficient primary porosity and conductivity for feasible groundwater extraction. In such areas, exploration is directed towards finding areas of increased transmissivity and storativity caused by secondary effects such as fracturing and weathering. In semi-arid regions, weathering concentrates along lines of structural weakness such as faults, fracture zones and dykes, which often

✉ Mohamed O. Arnous
arnous_72@yahoo.com; mohamed.arnous@science.suez.edu.eg

¹ Faculty of Science, Geology Department, Suez Canal University, Ismailia, Egypt

appear as linear features on satellite images, generally referred to as lineaments (Caruthers et al. 1991; Greenbaum 1992; Arnous et al. 2011; Arnous and Sultan 2014).

In the last several decades, Egypt has been subjected to a very arid climate, where there has been a remarkable increase in average temperature and decrease in rainfall intensity over the entire country. The water levels of the different aquifers have decreased with time and the springs of the different hydrographic basins have stopped flowing, for example at Wadi Hebran (Aggour 2006).

The hard rock of the Wadi Feiran basin (WFB), in South Sinai, is described as a fractured basement aquifer. Groundwater is the only source of water available to local inhabitants. Groundwater exploration and utilization, specifically in fractured basement rocks, needs an understanding of the geology, geological structures, geomorphology, climatic conditions and land-use/land-cover of an area, which directly or indirectly control the terrain characteristics (Mukherjee 1996; Ravindran and Jeyram 1997; Pradeep 1998; Kumar et al. 1999; Oh, et al. 2011; Elewa and Qaddah 2011; Pothiraj and Rajagopalan 2013; Mohamed et al. 2015).

The traditional approaches used to identify, delineate and map the groundwater potentiality (GWP) zones are mainly based on ground surveys using geophysical, geological and hydrogeological tools in addition to the geospatial technologies including remote sensing (RS) and geographic information system (GIS) investigation tools. The current methods of groundwater exploration utilizing geophysical and geo-electrical tools are expensive and time consuming; therefore, there is a need to exploit recent tools of RS and GIS in the exploration of groundwater (Sener et al. 2005 and Mohamed et al. 2015). Geospatial tools are rapid and cost-effective in producing and modelling valuable data in various geoscience and environmental research fields such as geology and geomorphology, and in the determination of slope and structural lineaments, land-use and land-cover. This helps in identifying and mapping the probable sites of GWP. Geospatial technologies have been used successfully to eliminate surface structures during mapping, and therefore represent an integral part of applied geomorphology (Verstappen 1977; Butler and Walsh 1998; Bocco et al. 2001; Bubenzer and Bolten 2008; Dar et al. 2010; Arnous 2011; Arnous and Green 2011; Arnous et al. 2011; Kuria, et al. 2012; Elmahdy 2012; Abdalla 2012; Pothiraj and Rajagopalan 2013; Arnous and Sultan 2014; Nampak, et al. 2014; Mallick et al. 2015; Arnous and Green 2015). There are a number of works where GWP has been estimated using geospatial technologies. Rao et al. (2009) carried out hydrogeological mapping coupled with hydrogeological investigations for evaluating GWP in Madhurawada, India, using GIS. Elewa and Qaddah (2011) mapped GWP zones in Sinai, Egypt, utilizing RS and GIS watershed-based modelling. Kamaraju et al. (1996) performed an evaluation of GWP of a district in India using GIS approaches. Shahid et al. (2000) employed GIS tools in the analysis of

hydrogeological data acquired from surface geophysical and RS techniques to assess the groundwater situation in Midnapur District of India.

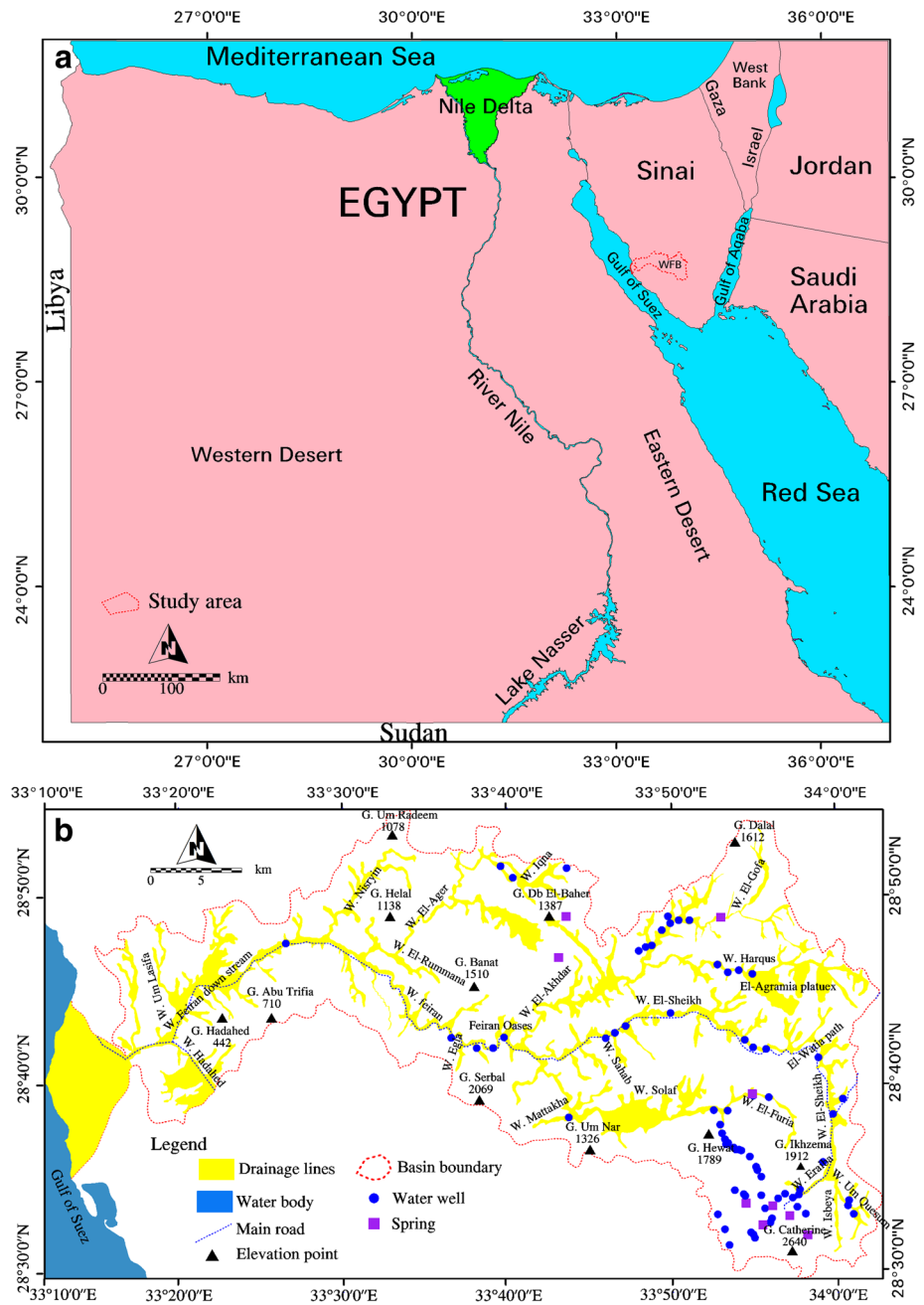
With the advent of RS and GIS tools, the mapping of GWP zones within each geological unit has become easier (Jain 1998; Singh and Prakash 2003; Abdalla 2012; Nag and Ghosh 2013). The groundwater conditions vary significantly based on numerous factors such as the slope, depth of weathering, structural lineaments, lithology, drainage density, plan curvature, topographic elevation and land forms. These factors can be interpreted or analyzed in GIS using RS data to indicate the GWP zones in qualitative terms. Many studies have used GIS and RS tools to prepare and analyze different thematic maps such as landforms, geomorphology, surface-water bodies, land-use, drainage pattern, lineaments, lithology, slope and soil (Krishnamurthy et al. 1996; Saraf and Choudhary 1998; Jaiswal et al. 2003; Solomon and Quiel 2006; Prasad et al. 2008; Chowdhury et al. 2009; Saha et al. 2010; Pareta and Pareta; 2011; Nag and Ghosh 2013).

The present study aims to delineate, identify and map GWP zones in arid terrain regions using RS data and a GIS approach to prepare various hydromorphogeological thematic maps such as slope, drainage density, lithology, landforms, structural lineaments, rainfall intensity and curvature, using ArcGIS. Additionally, groundwater-controlling factors will be assessed by combining RS, global digital elevation models (GDEM) and field study data with various thematic maps in a GIS modelling environment to create a groundwater prospect map of Wadi Feiran basin (WFB).

Study area

Wadi Feiran basin (WFB) is one of the important drainage systems in South Sinai. It is located between latitudes 28° 30' and 28° 55' north and longitudes 33° 20' and 34° 03' east and covers an area of approximately 1,868 km² (Fig. 1). WFB has the widest surface area of the many drainage basins that make up the drainage network of the Gulf of Suez. The main course of Wadi Feiran and its tributaries drain the surrounding high rugged mountains in the east (Abou El-Magd 2003). WFB trends slightly in the east to west direction and drains into the Gulf of Suez (Moneim 2005). Some villages along the main course of WFB have been prone to flash flood events once or twice annually, particularly in the autumn and spring seasons (Youssef et al. 2011). Rainfall represents the principal source of water supply. The WFB dissects a variety of rock units ranging in age from Precambrian to Quaternary (Abou El-Magd 2003; Youssef et al. 2011). The Feiran to Saint Catherine City road is located in the rugged landscape section and represents the primary access route to the St. Catherine area from the western side, while the eastern and southern parts of WFB are difficult to access except on foot (Abou El-Magd 2003; Youssef et al. 2011).

Fig. 1 a Location and b physiographic maps of Wadi Feiran basin (WFB) area, South Sinai, Egypt. Elevations in m asl



Geomorphologically, the highest peaks are located in the southern part of the WFB and are characterized by high-relief terrain such as Gabal (G.) Saint Catherin, G. Mussa, G. Serbal, G. Banat, G. Tarboush, and G. Mukattab; some of them reach 2,640 m asl (Fig. 1). The basement complex is composed mainly of strongly deformed Pre-Cambrian metamorphic and igneous rocks consisting largely of gneisses and granitic masses (Abou El-Magd 2003; Youssef et al. 2011). The Pre-Cambrian rocks are unconformably overlain by non-metamorphosed sediments, cropping out mainly in the north and west and covering about 20 % of the WFB.

It is very important to understand the climate of WFB, in order to understand and develop the concept of water budget and the hydrogeological conditions of the water resources. WFB is categorized by warm winters and hot summers. The mean values of minimum and maximum temperatures at the Catharine Weather Station are recorded as 13 and 34 °C, respectively. The annual relative humidity varies between 46 and 54 %. Precipitation in WFB is scarce and random; the average annual precipitation ranges between 1.6 and 21.5 mm. The highest recorded average annual rainfall in WFB is 76.2 mm (Egyptian Meteorological Authority 2006).

Materials and methods

Data used and image processing

Remote sensing (RS) is considered as a set of tools making possible the acquisition of information from space in a comprehensively visual way. Usually, RS data are used to provide information on terrain surface and suspicious signatures, as well as in monitoring approaches. GIS is considered a supporting technology to RS. It has the ability to manipulate, overly, integrate and store data in digital forms. These two technologies were employed in this research. RS and GIS techniques play essential roles in the spatial integration of various geo-datasets including OLI Landsat 8 satellite data, Advanced Spaceborne Thermal Emission and Reflection Radiometer (ASTER) data, and geological and geomorphological maps. GDEM data were utilized in this study to identify and also map the GWP zones and their environmental hazard impact by employed ArcGIS and ERDAS Imagine software. The OLI Landsat 8 images, dated 2014 for Path 175 and Row 40 and Path 174 and Row 40, covering the investigated area, have been radiometrically and geometrically corrected in UTM projection WSG84, with spatial resolutions of 28.5 and 14.25 m, respectively. Topographic maps of WFB acquired at scales of 1:50,000 and 1:100,000, a geological mapping by Conoco (EGPC/Conoco 1987) and the Geological map of Sinai by the Egyptian Geological Survey and Mining Authority (EGSMA 1994) were used as reference maps and have been digitally processed. A DEM was created from the ASTER GDEM and the topographic maps to analyze and map the topographic and the geomorphological terrain features, for instance slope, plan curvature, slope aspect, three-dimensional (3-D) view and elevation contour maps, as well as to investigate the geomorphological characteristics of the investigated area. Digital processing of the RS data created numerous products extending from single-band to stack image bands. False colour composite images, principal component analysis (PCA), band ratio, brightness inversion, directional filtering, IHA (intensity, hue and saturation) and histogram equalization techniques were all used for detecting and identifying the hydrogeomorphological potential parameters in the study area. The tabular data of rainfall (Tropical Rainfall Measuring Mission, TRMM) in the study area were used to support the processes of flood generation and groundwater recharge. The groundwater prospect map is based on multiple criteria, for instance, lithology, drainage texture, steepness of slope, geomorphology, frequency of lineaments, etc. All of these criteria were used at the same time as a multi-criteria evaluation.

Preparation of the geo-spatial thematic modelling and GWP maps

In order to identify, assess and generate the GWP map for the WFB, the main factors considered are slope degree, drainage

density, lithology, landforms, structural lineaments, structure density, rainfall, curvature, and elevation. The thematic maps of these factors were prepared and then converted into raster or vector form so that they could be easily integrated utilizing the GIS tool. Each of these constructed geo-spatial digital thematic maps has been given a suitable weight, which are based on the work carried out by researchers such as Krishnamurthy et al. 1996; Saraf and Choudhary 1998; Srinivasa and Jugran 2003; Sikdar et al. 2004; and Naghibi et al. 2015.

The thematic maps were then integrated using GIS tools to delineate GWP zones that are assigned knowledge-based hierarchy using the Spatial Analyst tool of ArcGIS. This required three steps: spatial database building, spatial data analysis and data integration. All geo-spatial thematic maps were re-classified and assigned suitable weights (Table 1). Multi-criteria evaluation was applied: the constructed geo-spatial maps of these parameters were assigned individual theme weights and class weights (Eastman 1999; Abdalla 2012; Arnous 2013). In this model, the thematic maps are ranked from 1 to 5, depending on their suitability to hold groundwater. The rank of each digital layer has been transformed into map weight by dividing each map ranked by the total number of ranks. Similarly, the map classes in each input map are assigned different categories and ranked by a numeric scale (1–5 where 5 is the most favorable and 1 is the least) based on the ability to reserve and transfer water. The rank of each inter-map class is divided by the total classes to generate the capability values (CV_i), as shown in Table 1. For example, the CV_i of the drainage density thematic layer for ranks one, two and three equals 1/6, 2/6 and 3/6 respectively (Table 1). These capability values are multiplied by the respective map weight in each thematic map to initiate the GWP zones map (Table 1). The procedure of linear combination dominates in raster files in the GIS software, and these files are assigned to produce a combined map (Eastman et al. 1995; Eastman 1999; Abdalla 2012). The individual theme weight (Table 1) was multiplied by its respective class weight and then all the geo-spatial thematic coverage data were combined in the weighted linear combination method and computed by the ArcMap GIS (Raster Calculator) module as a function of the Spatial Analyst tool to integrate it as given here:

$$W_i = Sp_w + Dd_w + Lt_w + Ld_w + Cr_w + Te_w + Lm_w + Rf_w \quad (1)$$

where W_i is map weight, Sp is the slope, Dd is the drainage density, Lt is the lithology, Ld is the lineament density, Cr is plan curvature, Te is the topographic elevation, Lm is the landform and Rf is the rainfall. The subscript w indicates the normalized weight of the individual features of each thematic layer.

$$GWP = \sum W_i \times CV_i \quad (2)$$

where the GWP is groundwater potential, W_i is map weight and CV_i is capability value (weight of inter-map class). Finally, the

Table 1 The thematic map weights and their capability values of WFB

Thematic layer	Map rank	Map weight (Wi)	Class ranges	Degree	Rank	Capability value (CVi)
Lithology	2	2/18 = 0.111	Metamorphic	Very low	1	0.06
			Older volcanic	Very low	1	0.06
			Older granitoids	Low	2	0.13
			Younger granitoids	Moderate	3	0.20
			Younger volcanic	Moderate	3	0.20
			Wadi deposits	High	4	0.26
			Sedimentary sequence	Very high	5	0.33
			Scarp landform	Very low	1	0.06
Landform	2	2/18 = 0.111	Lacustrine deposits	Low	2	0.13
			Highly rugged mountains basement complex	Moderate	3	0.20
			Peneplained surfaces	High	4	0.26
			Highly dissected tableland	High	4	0.26
			Inland alluvial fans	Very high	5	0.33
			Drainage system	Very high	5	0.33
			< 0.5	Low	1	0.1
			< 0.5–1.0	Moderate	2	0.2
Slope (degree)	3	3/18 = 0.166	< 1.0–1.5	High	3	0.3
			< 1.5	Very high	4	0.4
			≥ 15	Low	1	0.1
			< 15–10	Moderate	2	0.2
Curvature	2	2/18 = 0.111	< 10–5	High	3	0.3
			< 5–0	Very high	4	0.4
			> 0	Low	1	0.16
			0	Moderate	2	0.33
Topographic elevation (m)	1	1/18 = 0.055	< 0	High	3	0.5
			≥ 1,700	Low	1	0.1
			< 1,700–1,600	Moderate	2	0.2
			< 1,600–1,500	High	3	0.3
Drainage density (km/km ²)	2	2/18 = 0.111	< 1,500	Very high	4	0.4
			≤ 0.5	Low	1	0.16
			< 0.5–0.9	Moderate	2	0.33
			> 0.9	High	3	0.5
Rainfall data (mm)	3	3/18 = 0.166	≥ 0.03	Low	1	0.1
			< 0.03–0.05	Moderate	2	0.2
			< 0.05–0.07	High	3	0.3
			> 0.07	Very high	4	0.4

resultant GWP map is categorized into very poor, poor, moderate, good and very good GWP zones.

Validation of the constructed GWP map is the most important process of modeling in that without validation, the models will have no scientific significance. The validation was carried out by using water production rates from groundwater wells and geophysical data.

Results and discussion

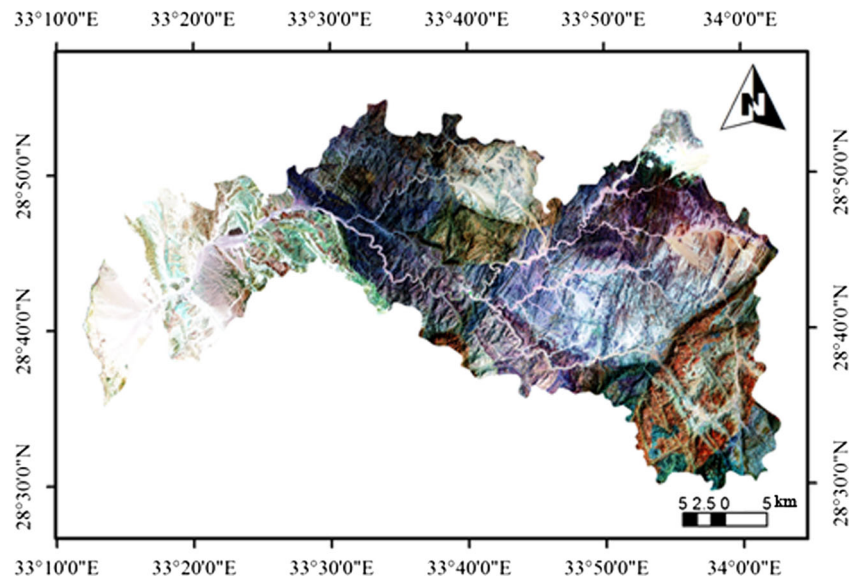
Lithological potential mapping

Water-bearing formations of the earth's crust act like conduits for transmission and like reservoirs for storing water. Surface runoff is usually high at sites of compact formations and very low at sites of loose and also more porous rocks, where the infiltration of the runoff water is controlled by the grain size and the porosity of the topsoil. These in turn are controlled by

rock hardness, weathering and the erosion mechanisms, lithology and also fracture spacing. Moreover, the presence of interconnected joints, fractures, cracks, crushed zones (for instance, fault or shear zones) or solution cavities, allows rainwater to easily infiltrate and recharge the groundwater (Todd 1980). In the current study, the lithological map of WFB area has been prepared with the help of OLI Landsat 8 satellite images and other published ancillary geological data.

A number of digital image processing techniques, including contrast stretching, PCA, brightness inversion, IHS and de-correlation stretch, were used to map rock types. The statistical technique assumed by Sheffield (1985) was used to select the most effective 'three-band colour composite' image. The band combination 7, 5 and 3 was used to create colour composites with OLI Landsat 8 data and assigned in red, green and blue, respectively. PCA and de-correlation stretch were also utilized to select the band combination and discriminate the differences between each rock unit (Fig. 2). The lithological units of WFB were mapped by using ArcGIS

Fig. 2 Contrast stretching enhanced OLI image of WFB area



and could be distinguished by distinct colour in the enhanced satellite images (Fig. 3). In the present study, ranging for lithological units is assigned depending on fractures, mineral assemblage, alteration and weathering conditions. The rock units that are highly fractured are more prone to weathering and have high infiltration and also high runoff resistance, and hence, high rank values were assigned. Likewise, the rock units that are less fractured and less prone to weathering are assigned low rank values. The lithological map of WFB was divided into five categories: (1) metamorphic rocks (biotite gneiss, calc-silicate gneiss, hornblende biotite gneiss, migmatites and metagabbro-diorite complex), (2) intrusive rocks (older granitoids, younger granitoids (phase II and III), (3) younger volcanic rocks (rhyodacite rutig, granophyre

dyke-like intrusions), (4) Phanerozoic sedimentary sequences, and (5) Quaternary deposits. Surface runoff is typically high in areas with massive, younger rocks and very slow in areas of friable, porous rocks (EGPC/Conoco 1987; EGSMA 1994). According to the runoff infiltration capability values of the lithological units of WFB, the study area is classified into five categories ranging from 1 for metamorphic rocks, old volcanics and granitoids to 4 for wadi deposits and 5 for sedimentary sequences (Table 1). Valley deposits are composed mostly of sand, silt and thick alluvium loose gravel that have large pores between the grains and easily allow surface water to infiltrate through the subsurface strata; thus, these valley deposits are highly favorable for GWP in addition to the highly weathered and fractured rock units of WFB.

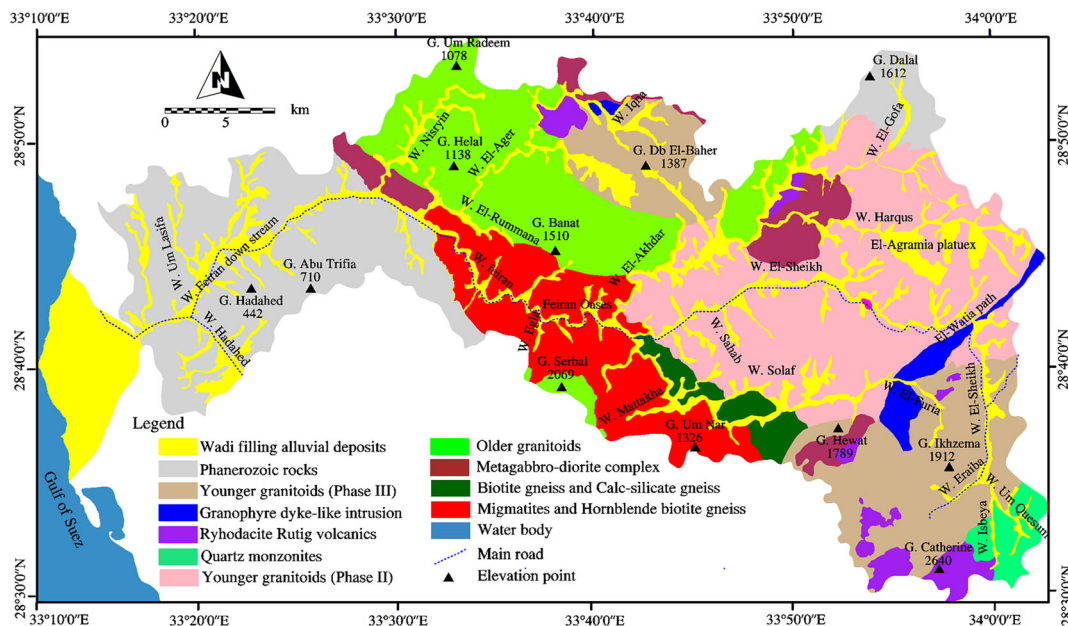


Fig. 3 Lithological map of WFB area

Hydrogeomorphological potential mapping

The geomorphology of an area is very important when evaluating the GWP (Kumar et al. 2008). In the current study, the hydrogeomorphological map is suitable for the planning and execution of groundwater exploration, in addition to clarifying controls on the movement and accumulation of surface water and groundwater. Topographic model parameters such as slope, elevation and curvature of the WFB were calculated from the ASTER GDEM and used for geomorphologic analysis. Moreover, the visual interpretation of the enhanced RS data is used to identify the different landform feature classifications of WFB. The geomorphological classification results were visually evaluated and re-classified into seven landform categories in order to construct the geomorphological map of WFB (Fig. 4). These classes include the highly rugged mountainous basement complex, highly dissected tableland, peneplained surfaces, inland alluvial fans, lacustrine deposits, drainage system and fault scarp landform classes (Table 1).

Structural lineaments potential mapping

Recently, RS has increasingly been applied, in both small-scale and regional investigations, to detect the structural lineaments and provide important information on surface and subsurface fracture systems (Hung et al. 2005; Dar et al. 2010; Arnous 2011; Arnous and Green 2011). The regional linear features that are surficial expressions of underlying structural features such as joints or faults in hard-rock areas, are considered to be good GWP zones, acting as good conduits for groundwater movement and zones of increased secondary porosity (Pradeep 1998; Obi Reddy et al. 2000;

Ganapuram et al. 2009). Areas up-gradient of dykes or other intrusions within a porous host rock often have good water potential, as the dyke/intrusive constitutes a barrier to groundwater flow. Lineaments have commonly been used as an indicative tool for locating GWP zones (Pradeep 1998; Obi Reddy et al. 2000; Ganapuram et al. 2009), but with the present scenario of over-exploitation of the aquifer (El-Rayes 2004; Dar et al. 2010), characterization of the structural lineament becomes essential to ensure the possibility of locating new GWP zones and managing over-exploited aquifers in hard rock areas. Structural lineaments are obvious in most enhanced OLI Landsat 8 satellite images. Most of the linear features of the study area can be eliminated by applying contrast-stretching techniques. Additionally, directional filtering was employed to different single band images of the OLI Landsat 8 images along NE–SW and NW–SE directions. Although major lineaments can be identified in the raw image data, most of the finer details are more clearly detectable in the filtered image after applying the directional filtering.

The GDEM was very useful in eliminating regional-scale structural lineaments related to geomorphologic features and drainage network channels; therefore, the shaded relief model is considered key in lineament extraction because it is the most suitable topographic terrain model to recognize and interpret complex geomorphologic features (Jordan et al. 2005; El-Rayes et al. 2015). In the current study, the shaded relief map was constructed from the GDEM by varying the azimuth and elevation of simulated sun illumination (Singh and Prakash 2003; Soulakellis et al. 2006; Arnous 2011; Arnous and Sultan 2014; El-Rayes, et al. 2015). The enhanced contrast stretching OLI Landsat 8 image of WFB (7, 5 and 3 as assigned RGB) colour composite was overlaid on the shaded

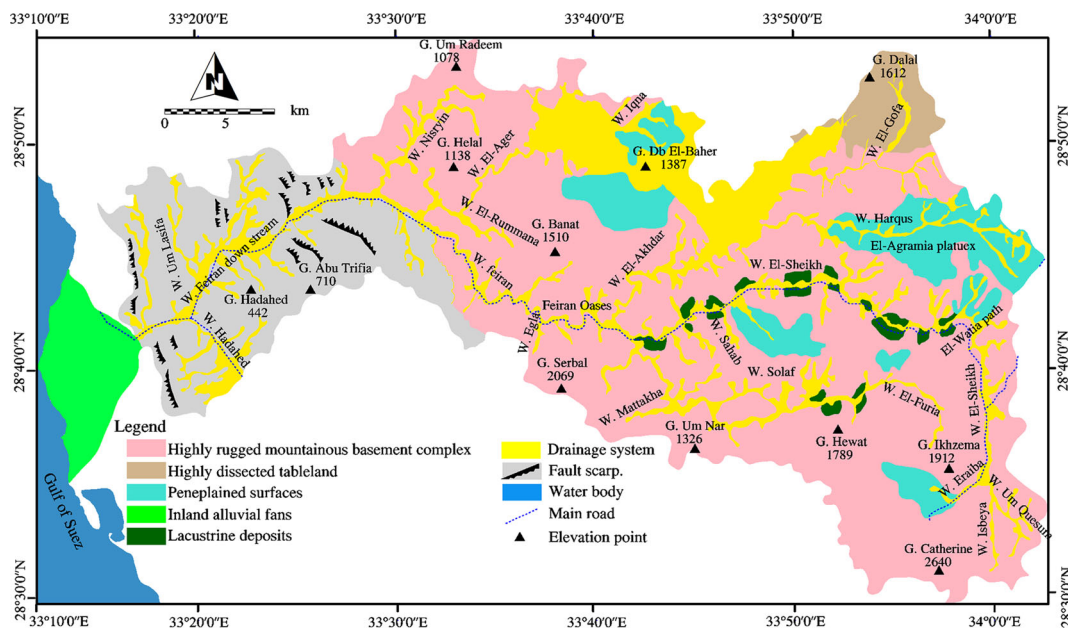


Fig. 4 Geomorphological map of WFB area

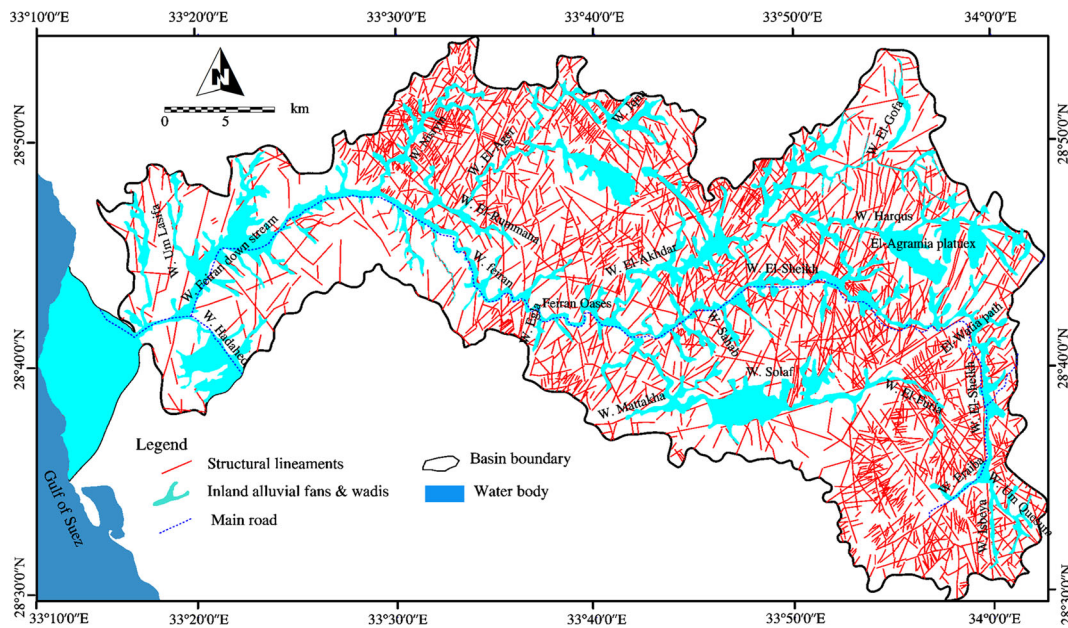


Fig. 5 Structural lineaments map of WFB area

relief maps to improve the manual detection and extraction of structural lineaments. The final integrated structural lineament map was constructed by combining all interpretations and editing duplicates in each of the files by using ArcGIS (Fig. 5). The majority of lineaments, such as fractures and faults, are oriented along NE–SW trends, while N–S and NW–SE trends are intermediate in magnitude and are dissected by the NE–SW trends.

The structural lineaments of WFB were converted into zones of different lineament density (lineaments per square km) and

rated as very high, high, moderate and low according to their capability for runoff infiltration and their significance with reference to their GWP (Table 1). The structure lineament density map (Fig. 6) shows that the younger crystalline rocks in WFB are highly fractured; however, the older volcanic rocks have a lower fracture density value or subdued anomalies, indicating that runoff water may penetrate and flow through the highly fractured younger lithological units rather than older lithological units of WFB. Finally, the asymmetry of lineament densities along the main valleys reflects the deformation history of the

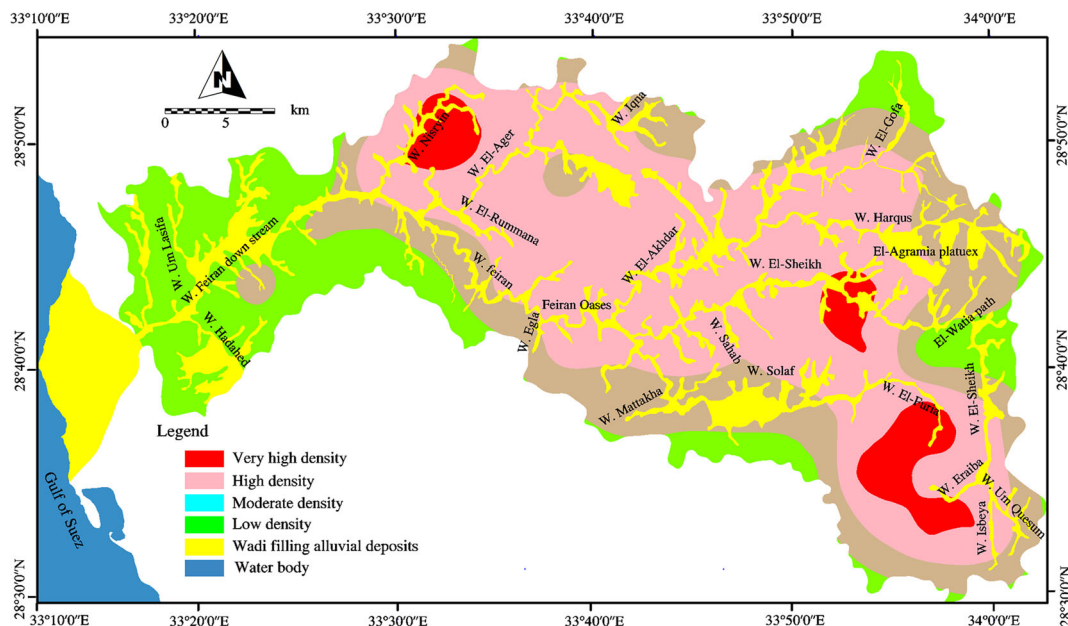


Fig. 6 Structural lineaments density map of WFB area

crystalline rocks. The study area is mainly covered by brittle rock types which respond quickly to compression stresses acting on the regional scale by fracturing (Mohamed et al. 2015). The structural lineaments act as conduits for groundwater flow, and hence are hydrogeologically significant, with GWP decreasing with increasing distance away from the lineaments. This indicates that the best chances for groundwater targeting are close to structural lineaments particularly in the hard crystalline rocks of WFB. The groundwater recharge in the investigated area finds its way through sets of interconnected joints to feed the existing wells in the low-lying fault zones (El-Rayes 2004; Solomon and Quiel 2006) and also discharges as springs along the contact between the weathered, fractured topmost rocks and the underlying fresh granites (El-Rayes 1992). According to this approach, the groundwater moves in a step-like downward flow until the fault zone is reached (El-Rayes 2004). These jointed and fractured rocks are dissected by NE–SW dikes, which also performance an important role in the groundwater occurrences in the fractured basement rocks and alluvium deposits (Abou El-Magd 2003; Aggour 2006).

Slope potential mapping

Slope is a function of the topographic surface and is calculated in ArcGIS using surface analysis within the Spatial Analyst tool. The occurrence and movement of groundwater is governed strongly by slope which is an important factor in runoff; the infiltration is inversely related to slope (Surabuddin et al. 2007; Arnous 2011; Arnous and Green 2011, 2015). The slope map of WFB (Fig. 7) has been prepared from the GDEM data range from flat (0°) to vertical (90°). The WFB area is classified into four zones (i.e., 0 to <5 , 5 to <10 , 10 to <15 , and ≥ 15). The slope

map indicates that the surface runoff is naturally slow in areas with gentle slope, allowing more time for rainwater percolation and promoting significant groundwater recharge. On the other hand, the steep slope areas support fast surface runoff, allowing less time for rainwater to infiltrate and recharge local groundwater aquifers. The southeastern and central parts of the study area have poor groundwater prospects due to high slope gradients; however, most of the valley floor has good groundwater prospects due to gentle slopes. GWP weights assigned to the slope categories are shown in Table 1.

Curvature potential mapping

The curvature values that are extracted from GDEM analysis by using ArcGIS in the WFB varies from -537.144 to $+555.138$, indicating that the hilly nature of the study area is oriented east–west. A positive curvature of WFB shows the surface is upwardly convex at that cell (flow dissipation zone), whereas a negative curvature of WFB shows the surface is upwardly concave (flow accumulation zone) and a value of zero indicates a flat surface and a flow transition zone (Fig. 8). In the results of WFB curvature, valleys and channels have the most negative values, while ridges have the most positive values. The curvature map was classified into three numerical ranks (Table 1) with reference to GWP weight. The GWP is much higher in the flat and highly negative curvature areas (Subba 2006; Elmahdy 2012). The class with a value of zero for curvature will give more potentiality for groundwater accumulation; moreover, areas showing the highly negative and flat values for curvature will exhibit low discharge of overland flow and high rates of infiltration, and have been assigned as high regarding GWP, whereas the positive value areas were considered poor for GWP.

Fig. 7 Slope degree map of WFB area

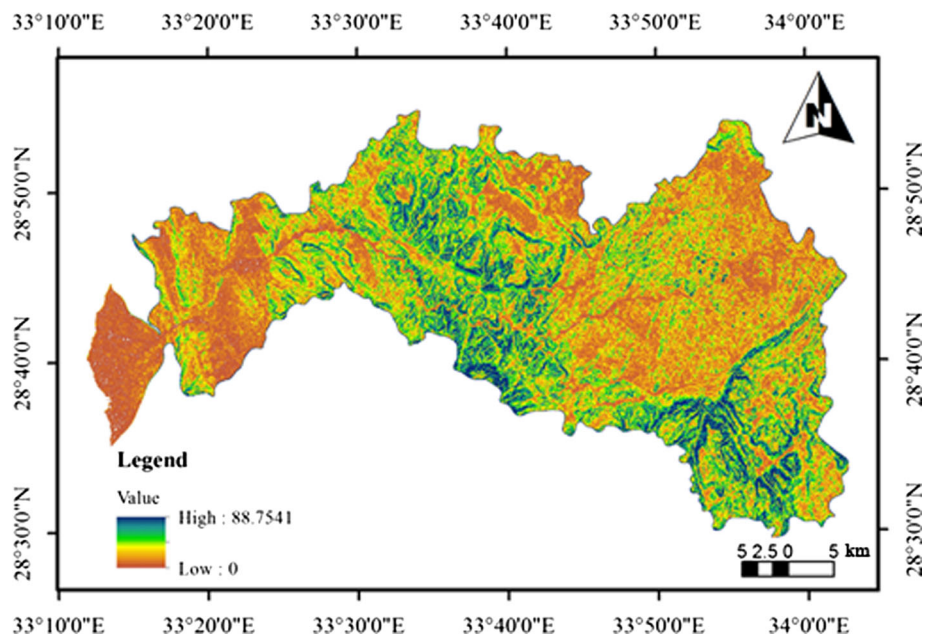
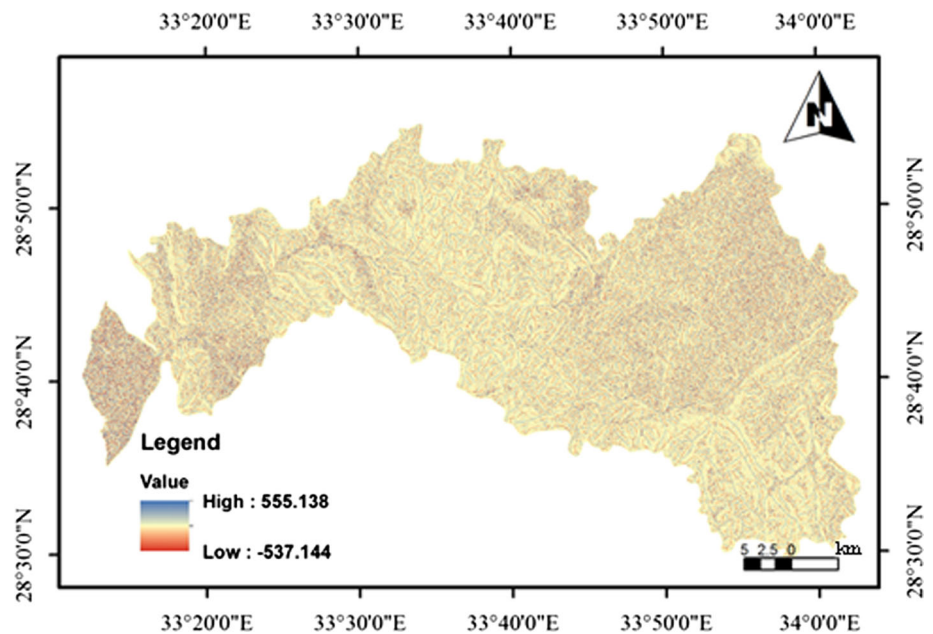


Fig. 8 Curvature (radians per meter) map of WFB area



Topographic potential mapping

Surface topography determines the flow direction of runoff water over the ground surface, and it has a great influence on groundwater occurrence, in that the steepness of slope increases runoff and therefore decreases potential recharge. The topographic conditions of the WFB area control the groundwater flow particularly in fractures and overland flow. The depth to water table in the existing hand dug wells varies widely due to the local topography (Ghodeif 1995). The local slope affects mainly the quantity of infiltration and the rate of overland flow, since the steep slopes allow less time for infiltration and increase the surface runoff. Wadi Feiran ASTER GDEM was employed to analyze the topographic elevation zones in WFB. The GDEM analysis result revealed that the ground surface elevation ranges from 1 to 2,607 m asl. The irregular variations between highest and lowest zones generate slopes that control the water movement to the west and the Gulf of Suez, whereas the basement rocks of WFB occupy the highest topographic levels to the east. The elevation density map was constructed by classifying the GDEM into four numerical categories (i.e. $\geq 1,700$, $<1,700-1,600$, $<1,600-1,500$, $<1,500$) based on their infiltration potentiality of runoff water (Fig. 9). The values range from low to very high based on their significance to groundwater recharge potential (Shendi and Abou El-Magd 2004; Abou El-Magd 2003)—ranks 1, 2, 3, and 4 assigned are low, moderate, high, and very high respectively (Table 1).

Drainage potential mapping

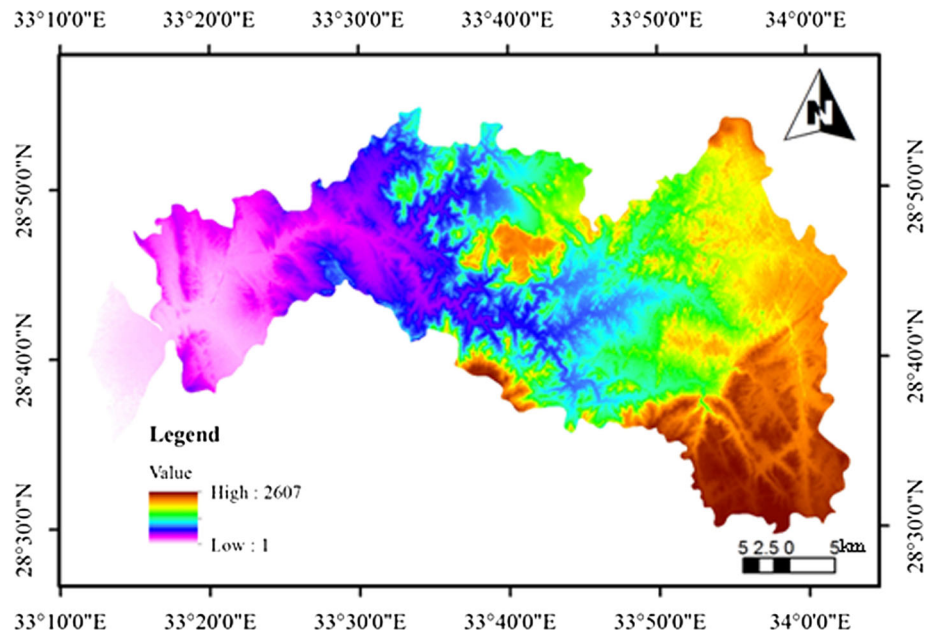
WFB represents the main drainage basin, in which the Wadi Feiran discharges its water into the Gulf of Suez. The drainage

pattern of WFB and its watershed map has been extracted from the GDEM data by using the flow direction algorithm of Jenson and Domingue (1988). Flow direction will permanently be in the steepest down-slope direction and also is used to define the stream network. The flow direction map of WFB produced from a raster shows that the flow direction of WFB is from east to west to the Gulf of Suez. The raster of flow accumulation of WFB indicates that the low accumulation values characterize ridge tops, whereas higher accumulation values represent stream channels and also valleys. The drainage patterns observed in the WFB are dendritic, trellis, rectangular and parallel, and the WFB has a drainage density of 2–13 km/km². Stream ordering was identified by using DEM and drainage network in the Hydrology module of ArcGIS (Fig. 10). The drainage network helps in the delineation of watersheds and for suggesting various water-harvesting structures and soil conservation measures. The drainage density map was calculated from the GDEM-derived drainage channel network to define zones of different drainage density (Fig. 11), and the WFB area was divided into three numerical categories based on the capability of recharge infiltration (Table 1); furthermore, the produced drainage density map revealed that the areas of high density reflected a low chance for groundwater recharge and vice versa.

Rainfall intensity potential mapping

Rainfall represents the main source of the groundwater recharge in WFB. At times, rain produces floods along the main streams or wadis that commonly flow towards the west direction. On the other hand, a considerable amount of the rainfall percolates into the basement terrain through open spaces and fracture

Fig. 9 Topographic elevation (m asl) map of WFB area



systems. Water moves downward through the fractures by both hydraulic gradient and gravitational forces to recharge both Phanerozoic sedimentary rocks and the Quaternary alluvial deposits; therefore, it is more useful to classify the water-bearing formations beginning with the fractured basement rocks followed by the Quaternary alluvial deposits and then the Pre-Cenomanian aquifer (Abou El-Magd 2003).

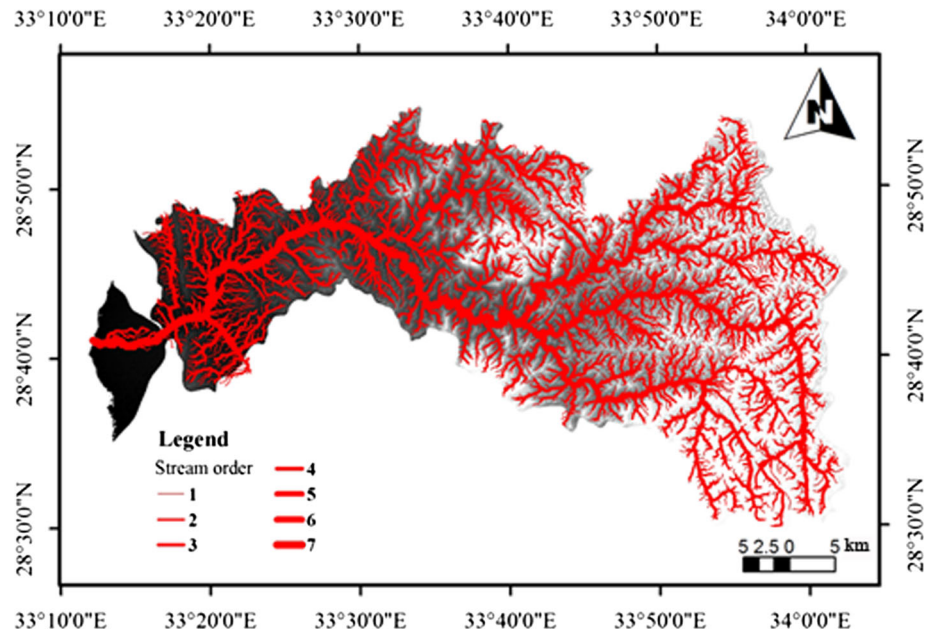
Today, Tropical Rainfall Measuring Mission (TRMM) data provide important information on rainfall impact along the drainage network systems globally. These data are helpful in predicting flash flood hazards, and estimating the runoff volume of surface water. The TRMM data on WFB are

interpolated and categorized into four categories; low, moderate, high and very high by using ArcGIS (Fig. 12). The area of highest rainfall anomaly is located in the east of WFB particularly at G. Saint Catherine. The classes are assigned weight factors of 1, 2, 3 and 4 that are low, moderate, high and very high respectively (Table. 1).

Spatial modelling and data integration of GWP zones

One of the most important applications of geo-spatial tools is the mapping, analysis and integration of geo-spatial data to support the process of environmental decision-making. A

Fig. 10 Drainage map of WFB area



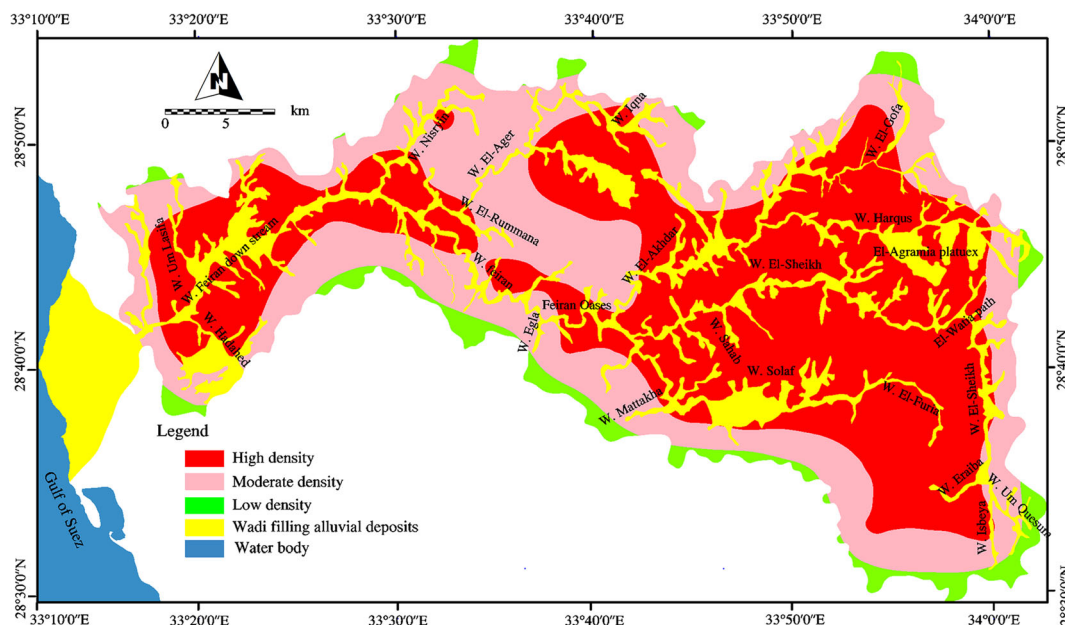


Fig. 11 Drainage density map of WFB area

decision can be well defined as a choice between alternatives, where the alternatives might be different locations, actions, objectives, and the like. In the present study, the RS and GIS data of WFB are integrated to delineate the areas most suitable for groundwater prospecting in this arid region of hard rock terrain. The geospatial tools have been successfully used to identify and eliminate areas, and to create spatial distribution maps of the possibilities of groundwater accumulation, based on lithology, structure, slope, curvature, landforms, topography, rainfall and drainage network data analyses. Consequently, a groundwater prospect map was constructed

by using a linear combination of these factors in an ArcGIS spatial analysis environment. The groundwater prospect map of WFB was classified into five categories from very high to very low probabilities of GWP zones (Fig. 13). The numerous geo-spatial thematic maps as described in the preceding have been transformed into raster form. These were then reclassified and assigned suitable weights following the methods used by Krishnamurthy et al. (1996), Saraf and Choudhary (1998) and Srinivasa and Jugran (2003).

The final cumulative groundwater prospect map was formed by applying the linear combination equations of the

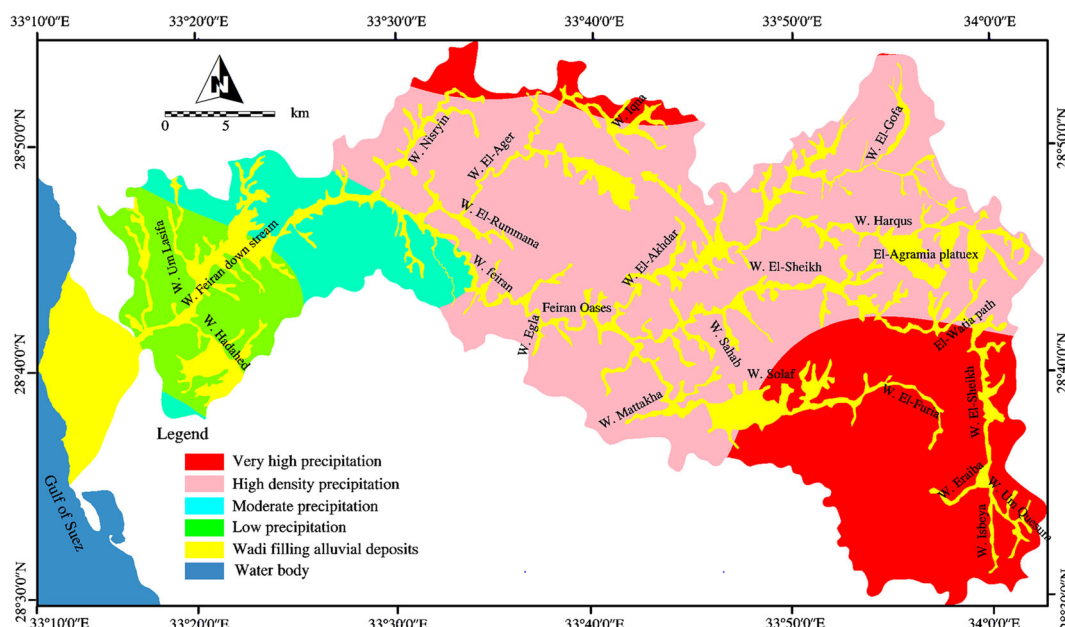


Fig. 12 Rainfall potential map of WFB area, based on TRMM data (1998–2013)

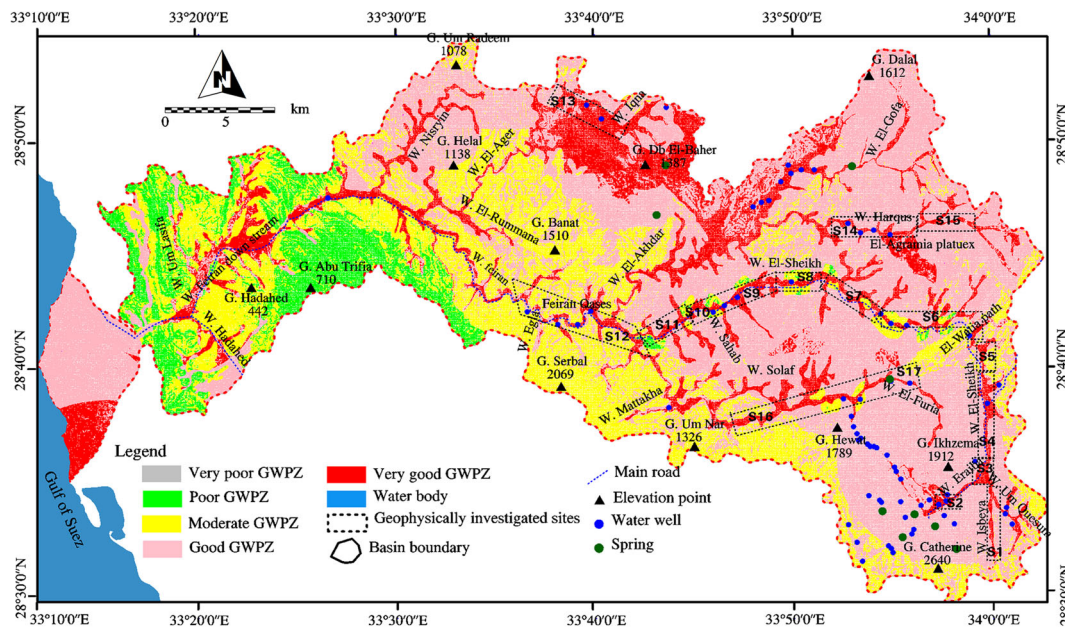


Fig. 13 Integrated spatially distributed groundwater potential zones (GWPZ) and locations of wells, springs and previous geophysical measurements in the WFB area

multi-criteria evaluation model with weight values ranging from 0.01 to 1.5. The very good and good areas occupied about 67.21 % of the total area which represents valley deposits, sedimentary sequences and areas of younger basement rocks (Table 2). The deeply weathered metamorphic and older basement rocks, characterized by moderate to very poor zones, represent about 32.79 % of the total area. From a hydrogeological point of view, none of the hard rocks have sufficient primary porosity for any significant groundwater storage. The rocks are, however, extensively tectonized and a large number of fracture zones intersect the terrain.

The water demand in the study area is high and many groundwater investigations have been carried out during the last few decades. Generally, structural lineaments act as conduits for groundwater flow, and are therefore hydrogeologically significant. The values allocated to structural lineaments were dependent on the relation of well yields to proximity of the lineaments. Four classes were defined based on distance from structural lineaments, with decreasing values as the distance from lineaments increases, assuming that the GWP decreases with increasing distance away from

the lineaments. This implies that the best chances for groundwater targeting are close to structural lineaments (Solomon and Quiel 2006).

Areas displaying negative values for plan curvature were assigned good potential, whereas areas with positive values were described as poor for GWP. The modelling results of the present study make it feasible to predicate locations of probable groundwater recharge in arid terrain regions. Ancillary geophysical analyses and field observations validated the GWP zones map; furthermore, compared with the ancillary published groundwater well data, data that were collected from the field support the conclusion of high yields particularly in the favorable zones that are extracted from RS and GIS integrated data. These favorable zones originated as valley beds where there is a thick accumulation of sand and gravel in addition to deeply fractured and weathered basement rocks.

Validation of the GWP zone map of WFB

Validation is considered to be the most important process of modelling. Without verification, models have no scientific

Table 2 The distribution of groundwater potential zones in WFB

Prospective zone	Area (km ²)	Area (%)	Weight	Class
1 (Very low groundwater potential)	17.50	0.94	0.01–0.3	Very poor
2 (Low groundwater potential)	127.65	6.84	0.3–0.6	Poor
3 (Moderate groundwater potential)	467.20	25.01	0.6–0.9	Moderate
4 (High groundwater potential)	946.12	50.65	0.9–1.2	Good
5 (Very high groundwater potential)	309.33	16.56	1.2–1.5	Very good

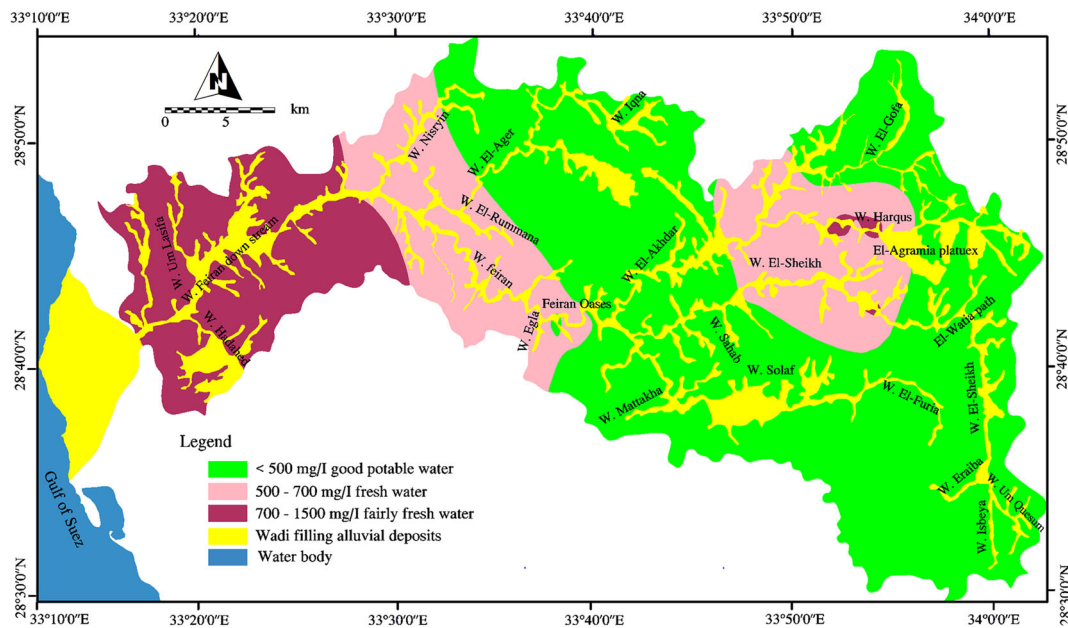


Fig. 14 Groundwater salinity distribution map of WFB area

significance (Chang-Jo and Fabbri 2003). The GWP map of WFB area was verified by correlating the potential classes with the spatial distribution of the productive wells and sites (previously investigated) by using various geophysical tools. The groundwater potentiality data such as topography, number of wells, well yield and groundwater depth, were collected from a literature review and were used for cross validation and confirmation of the GWP modelling results. Eighty-three individual groundwater wells and springs distributed in different water bearing formations of WFB were used to delineate the best potential zones for groundwater extraction. The groundwater data on the existing productive wells were collected from dug wells, drilled wells and springs, along with their geographic location. Production rates of wells were calculated based on transmissivity values that were obtained from pumping and recovery tests such as those of Haroun well at 109.8 m³/day; 1,872.8 m³/day at El-Watia well and 330.5 m³/day at Feiran-2 well (El-Refaei 1992; El-Rayes 1992; Abou El-Magd 2003).

The GWP map is overlaid with the spatial distribution of the groundwater wells and the cumulative percentage of the groundwater occurrence of the study area (Fig. 13). The overlaid maps show that there is a positive correlation between groundwater well locations and the GWP area, whereas the well locations with low productivity and areas without wells coincided with the sites falling into poor GWP classes. The groundwater well locations with high productivity coincided with the sites falling in the very good and good GWP classes particularly at W. Harqus, W. El-Sheikh, W. El-Furia, W. El-Akhdar and Saint Catherine sites. These wells were located through the valley alluvial deposits (Quaternary aquifer); moreover, the bottom of these wells is close to barrier rocks

like massif hard rocks, which hinder water infiltration to greater depths (El-Rayes 1992). The yield of these wells has been found to vary from 11.5 to 1872.8 m³/day. The water quality is good or acceptable and the salinity ranges from 228 to 1,071 ppm (Abou El-Magd 2003). This variation of WFB salinity follows the groundwater flow direction from east to west along the main stream from the recharge to the discharge areas (El-Sayed et al. 2012; Fig. 14). Local farmers have been using shallow groundwater from the Quaternary strata to irrigate several crops at the entrance of WFB particularly at Feiran and Tarfa Oases. Additionally, there are wells that fit the very good and good zones, although they are located in the elevated areas. These pertain to other factors such as fractured rocks that act as conduits for the water infiltration and accumulation.

From the hydrogeological point of view, many geophysical studies have been carried out in WFB area such as Wachs et al. 1979; El-Shazly et al. 1985; Awad and Armanious 1985; Shendi 1989; Hosney 1991; Shendi 1992; Shendi and El-Rayes 1992; Abou El-Magd 2003. Most of these studies have been carried out in different parts of WFB to study the GWP and by applying different methods including electrical resistivity, seismic refraction and magnetic techniques. The location of the geophysical measurements (Fig. 13) shows that there is a positive correlation between geophysical measurements sites and the good GWP zones. The geophysical measurements from previous work at sites S1–S17 coincided with the very good to good GWP zones of WFB. The literature review of the geophysical measurements revealed good information and examples in Wachs et al. (1979) who investigated the groundwater in Saint Catherine at site S7 using seismic refraction and electrical resistivity methods. They concluded that the recharge of valley fill is derived mainly from the joints system of the

bedrock and only partially from flooding. In addition, they showed that the jointed, saturated bedrock has a lower resistivity and higher seismic velocity than unjointed crystalline rocks. El-Shazly et al. (1985) evaluated the GWP in the Saint Catherine area by applying a resistivity method (site S6), whereby they revealed that groundwater exists mainly in the bottom of the wadi and in fractured basement rocks in several isolated basins. Awad and Armanious (1985) studied the GWP at El-Wet El-Agramia area by applying an electrical resistivity method (S14 and S15). They concluded that the thickness of the alluvium varies from a few meters to about 20 m, and although the quantity of water was expected to be poor, its quality was expected to be good. Shendi (1989) located new sites for promising water wells at two locations at Bir Zituna and Wadi Solaf at site S16 by applying a combination of magnetic and vertical electrical sounding techniques. The interpreted results revealed remarkable irregularities in the basement surface below the wadi fill in the Wadi Solaf area, and that these irregularities might act as limited basins for groundwater storage. In addition, Shendi (1992) applied magnetic and geoelectric sounding and seismic refraction to determine the thickness and physical properties of the alluvial deposits and to prospect the groundwater resources in El-Agramia plain at site S15. Shendi (1992) suggests two locations for drilling water wells and constructing surface dams to increase the productivity of groundwater. Shendi and El-Rayes (1992) searched for groundwater resources in the basement terrain of the Saint Catherine area by using magnetic and geoelectric sounding and seismic refraction techniques. They concluded that groundwater was present mainly in the bottom part of the alluvium and in the weathered top part of the basement bedrock; consequently, they recommended two locations along Wadi El-Sheikh for drilling new production water wells, at sites S1 and S4. Moreover, Abou El-Magd (2003) used magnetic measurements and geoelectric soundings at different sites to map the basement surface relief underlying the alluvial deposits, to delineate sub-surface geoelectric layers, to estimate their thicknesses and depths, and to determine the lateral and vertical extensions of both the alluvial aquifer and the underlying weathered basement aquifer (sites S2, S3, S5, S8, S9, S14 and S17).

Finally, based on the verification of the GWP zone map, there is a need to plan and design suitable water conservation measures in the WFB such as multiple traditional dams, spreader dikes and cisterns to be used to increase the infiltration rate and to store or conserve runoff water especially along the very good GWP zones. Multiple dams may play a powerful role on decreasing the runoff velocities and mitigate flash flood hazards. As a lot of water is needed to saturate the thick alluvial cover along the main stream of the very good GWP zones, direct artificial groundwater recharge through wide dug wells is recommended, particularly in areas of high field capacities such as the downstream sections of W. Solaf, W. El-

Sheikh, W. El-Ager and W. El-Akhader. Moreover, artificial recharge may positively change the water budget of WFB by stabilizing the volume of water that infiltrates and recharges the aquifers.

Shallow groundwater of WFB is subjected to potential contamination by surface contaminants. Such contaminants get into shallow large-diameter dug wells by being washed in during the heavy rains. Mitigation measures should be considered in well design to prevent the arrival of contaminants to the well water. The well head should be designed high enough to protect the groundwater inside the well.

Conclusions

Geospatial tools have been successfully used to identify and eliminate areas, and to create spatial distribution maps of the possibilities of groundwater accumulation in hard rock terrain of the arid WFB region. Weighted potential maps were prepared for lithology, structure, slope, curvature, landforms, topography, rainfall and drainage network data analyses. Consequently, a groundwater prospect map was constructed by using a linear combination of factors in a raster-based ArcGIS spatial analysis environment. The integrated result was classified into four categories from high to low probability GWP zones.

This result demonstrates that it is feasible to predicate locations of probable groundwater accumulation in arid hard-rock terrain regions. Ancillary geophysical analyses and field observations validated the GWP zones map; furthermore, comparison with the published groundwater well data support the prediction of considerable yields in the favorable GWP zones that are extracted from RS and GIS integrated data. These favorable zones are distributed along the valley alluvium deposits where there is a thick accumulation of sand and gravel intercalations in addition to the deeply fractured and weathered basement rocks. The results of this integrated WFB model suggests a need to employ, plan and design suitable water conservation measures to increase infiltration rates and store or conserve runoff water especially along the very good GWP zones. As part of this, multiple dams may play a powerful role in decreasing the runoff velocities along the very good GWP zones and in mitigating flash flood hazards. Direct artificial groundwater recharge of the thick alluvial cover along the main stream of the very good GWP zones through wide dug wells is recommended, particularly in down-stream areas of high field capacity. This may positively change the water budget of WFB by increasing the volume of water that infiltrates and recharges the aquifers there. Finally, the well heads at ground surface of WFB should be designed high enough to prevent the arrival of contaminants during the heavy rains and to protect the water inside the well.

Acknowledgements The author wishes to express his appreciation and gratitude to Prof. Ahmed E. El-Rayes, Geology Department, Faculty of Science, Suez Canal University, Egypt, for his constructive criticism on an earlier draft of the manuscript and his fruitful discussions. The author thanks reviewers Timothy Evans, Graham Jenke and the editor of *Hydrogeology Journal* for giving constructive comments that also helped improve the manuscript.

References

- Abdalla F (2012) Mapping of groundwater prospective zones using remote sensing and GIS techniques: a case study from the Central Eastern Desert, Egypt. *J African Earth Sci* 70:8–17
- Abou El-Magd AA (2003) Quantitative hydrogeological studies on Wadi Feiran Basin, South Sinai, with emphasis on the prevailing environmental conditions. MSc Thesis, Suez Canal University, Ismailia, Egypt, 252 pp
- Aggour TA (2006) Water resources of Wadi Feiran with emphasis on geomorphology and geology. *Ann Geol Surv Egypt V(XXIX)*: 357–387
- Amous MO (2011) Integrated remote sensing and GIS techniques for landslide hazard zonation: a case study Wadi Watier area, South Sinai, Egypt. *J Coast Conserv* 15(4):477–497. doi:10.1007/s11852-010-0137-9
- Amous MO (2013) Geotechnical site investigations for possible urban extensions at Suez City, Egypt using GIS. *Arab J Geosci* 6:1349–1369. doi:10.1007/s12517-011-0441-1
- Amous MO, Green DR (2011) GIS and remote sensing as tools for conducting geo-hazards risk assessment along Gulf of Aqaba coastal zone, Egypt. *J Coast Conserv* 15(4):457–475. doi:10.1007/s11852-010-0136-x
- Amous MO, Green DR (2015) Monitoring and assessing waterlogged and salt-affected areas in the Eastern Nile Delta region, Egypt, using remotely sensed multi-temporal data and GIS. *J Coast Conserv* 19(3):369–391. doi:10.1007/s11852-015-0397-5
- Amous MO, Sultan YM (2014) Geospatial technology and structural analysis for geological mapping and tectonic evolution of Feiran-Solaf metamorphic complex, South Sinai, Egypt. *Arab J Geosci* 7: 3023–3049. doi:10.1007/s12517-013-0959-5
- Amous MO, Aboulela HA, Green DR (2011) Geo-environmental hazards assessment of the north western Gulf of Suez, Egypt. *J Coast Conserv* 15(1):37–50. doi:10.1007/s11852-010-0118-z
- Awad WK, Armanious GM (1985) Geoelectric study at El-Wat El-Agramia, Saint Catherine area, Sinai, Egypt. *Ann Geol Surv Egypt XV*:317–323
- Bocco G, Mendoza M, Velazquez A (2001) Remote sensing and GIS-based regional geomorphological mapping: a tool for land use planning in developing countries. *Geomorphology* 39:211–219
- Bubbenzer O, Bolten A (2008) The use of new elevation data (SRTM/ASTER) for the detection and morphometric quantification of Pleistocene megadunes (Draa) in the eastern Sahara and the southern Namib. *Geomorphology* 102:221–231
- Butler DR, Walsh SJ (eds) (1998) The application of remote sensing and geographic information systems in the study of geomorphology. *Geomorphology* 21(3–4):179–349
- Caruthers RM, Greenbaum D, Peart RJ, Herbert R (1991) Geophysical investigations of photolineaments in southeast Zimbabwe. *Q J Eng Geol* 24:437–451
- Chang-Jo F, Fabbri AG (2003) Validation of spatial prediction models for landslide hazard mapping. *Nat Hazards* 30(3):451–472
- Chowdhury A, Jha MK, Chowdhury VM, Mal BC (2009) Integrated remote sensing and GIS-based approach for assessing groundwater potential in West Medinipur district, West Bengal, India. *Int J Remote Sens* 30:231–250
- Dar IA, Sankar K, Dar MA (2010) Remote sensing technology and geographic information system modelling: an integrated approach towards the mapping of groundwater potential zones in hardrock terrain, Mamundiyyar. *J Hydrol* 394:285–295
- Eastman JR (1999) Multi-criteria evaluation and GIS. In: Longley PA, Goodchild MF, Maguire DJ, Rhind DW (eds) *Geographical information systems*, chap 35. Wiley, New York, pp 493–502
- Eastman JR, Jin W, Kyem PAK, Toledano J (1995) Raster procedures for multi-criteria/multi-objective decisions. *Photogrammet Eng Remote Sens* 61:539–547
- EGPC/Conoco (1987) Photogeological interpretation map, scale (1: 100, 000). CORALI, Cairo
- EGSMA (1994) Geological map of Sinai, sheet no. 1, scale 1:250000, Geological Survey of Egypt, Cairo
- Egyptian Meteorological Authority (2006) Climatic atlas of Egypt. Ministry of Transportation and Communications, Cairo
- Elewa HH, Qaddah AA (2011) Groundwater potentiality in Sinai Peninsula, Egypt, using remote sensing and GIS-watershed-based modelling. *Hydrogeol J* 19:613–628. doi:10.1007/s10040-011-0703-8
- Elmahdy SI (2012) Hydromorphological mapping and analysis for characterizing Darfur Paleolake, NW Sudan using remote sensing and GIS. *Int J Geosci* 3:25–36
- El-Rayes AE (1992) Hydrogeologic assessment of St. Catherine area, South Sinai. 3rd Conf. Geology of Sinai for Development, Ismailia, Egypt, December 1992, pp 273–280
- El-Rayes AE (2004) Use of lineament analyses and joint measurements as guides for drilling high yield water wells in the basement aquifer of south Sinai. *JMPE* 7(1):67–76
- El-Rayes AE, Amous MO, Aboulela HA (2015) Hydrogeochemical and seismological exploration for geothermal resources in South Sinai, Egypt utilizing GIS and remote sensing. *Arab J Geosci* 8:5631–5647. doi:10.1007/s12517-014-1667-5
- El-Refaei AA (1992) Water resources of southern Sinai, Egypt. PhD Thesis, Cairo Univ., Cairo, Egypt, 357 pp
- El-Sayed MH, Abo El-Fadl MM, Shawky HA (2012) Impact of hydrochemical processes on groundwater quality, Wadi Feiran, South Sinai, Egypt. *Austr J Basic Appl Sci* 6(3):638–654
- El-Shazly MM, Mohamed SS, Abd-Alatif TA, Misak RF, Mabrouk MA (1985) Groundwater potential of St. Katherine Monastery environs, Sinai. *Egypt J Geol* 29(1–2):89–100
- Ganapuram S, Kumar GTV, Krishna IVM, Ercan K, Demirel MC (2009) Mapping of groundwater potential zones in the Musi basin using remote sensing data and GIS. *Advan Eng Soft* 40(7):506–518
- Ghodeif K (1995) Hydrogeological studies on the east St. Katherine environs, south central Sinai, Egypt. MSc Thesis, Suez Canal University, Ismailia, Egypt, 180 pp
- Greenbaum D (1992) Structural influences on the occurrence of groundwater in SE Zimbabwe. In: Wright EP, Burgess WG (eds) *Hydrogeology of crystalline basement aquifers in Africa*. *Geol Soc Spec Publ* 66:77–85
- Gustafsson P (1994) SPOT satellite data for exploration of fractured aquifers in a semi-arid area in southeastern Botswana. *Appl Hydrogeol* 2:9–18
- Hosney HM (1991) Detailed seismic refraction and resistivity measurements around a dyke in St. Katherine area, southern Sinai, Egypt. *Bull Fac Sci Ain Shams Univ* 28B:491–512
- Hung L, Batelaan O, De Smedt F (2005) Lineament extraction and analysis, comparison of LANDSAT ETM and ASTER imagery: case study—Suoimuoi tropical karst catchment, Vietnam. *Remote Sens Int Soc Optic Photon* 59830T-59830T-12. In: *SPIE Proceedings*, vol 598, SPIE, Bellingham WA

- Jain PK (1998) Remote sensing techniques to locate ground water potential zones in upper Urmil River basin, District Chhatarpur-Central India. *J Ind Soc Remote Sens* 26(3):135–147
- Jaiswal RK, Mukherjee S, Krishnamurthy J, Saxena R (2003) Role of remote sensing and GIS techniques for generation of groundwater prospect zones towards rural development: an approach. *Int J Remote Sens* 24:993–1008
- Jenson SK, Domingue JO (1988) Extracting topographic structure from digital elevation model data for geographic information system analysis. *Photogrammet Eng Remote Sens* 54:1593–1600
- Jordan G, Meijninger BMI, Van Hinsbergen DJJ, Meulenkamp JE, Van Dijk PM (2005) Extraction of morphotectonic features from DEM's: development and applications for study areas in Hungary and NW Greece. *Int J Appl Observ Geoinformat* 7:163–182
- Kamaraju MVV, Bhattacharya A, Reddy GS, Rao GC, Murthy GS, Rao TCM (1996) Ground-water potential evaluation of West Godavari District, Andhra Pradesh State, India: a GIS approach. *Ground Water* 34(2):318–325
- Krishnamurthy JN, Venkatesa K, Jayaraman V, Manivel M (1996) An approach to demarcate ground water potential zones through remote sensing and geographical information system. *Inter J Remote Sens* 17:1867–1884
- Kumar A, Tomar S, Prasad LB (1999) Analysis of fractured inferred from DBTM and remotely sensed data for groundwater development in Godavari sub-watershed, Giridih, Bihar. *J Indian Soc Remote Sens* 26(2):105–114
- Kumar MG, Agarwal AK, Bali R (2008) Delineation of potential sites for water harvesting structures using remote sensing and GIS. *J Indian Soc Remote Sens* 36(4):323–334
- Kuria DN, Gachari MK, Macharia MW, Mungai E (2012) Mapping groundwater potential in Kitui District, Kenya using geospatial technologies. *Int J Water Resour Environment Eng* 4(1):15–22
- Mallick J, Chander Kumar Singh CK, Al-Wadi H, Ahmed M, Rahman A, Shashtri S, Mukherjee S (2015) Geospatial and geostatistical approach for groundwater potential zone delineation. *Hydrol Proc* 29(3):395–418
- Mohamed L, Sultan M, Ahmed M, Zaki A, Sauck W, Soliman F, Yan E, Elkadiri R, Abouelimged A (2015) Structural controls on groundwater flow in basement terrains: geophysical, remote sensing, and field investigations in Sinai. *Surv Geophys*. doi:10.1007/s10712-015-9331-5
- Moneim AAA (2005) Overview of the geomorphological and hydrogeological characteristics of the Eastern Desert of Egypt. *Hydrogeol J* 13(2):416–425
- Mukherjee S (1996) Targeting saline aquifer by remote sensing and geophysical methods in a part of Hamirpur–Kanpur, India. *Hydrogeol J* 19:53–64
- Nag SK, Ghosh P (2013) Delineation of groundwater potential zone in Chhatna Block, Bankura District, West Bengal, India using remote sensing and GIS techniques. *Environ Earth* 70:2115–2127
- Naghibi SA, Pourghasemi HR, Pourtaghi ZS, Rezaei A (2015) Groundwater qanat potential mapping using frequency ratio and Shannon's entropy models in the Moghan watershed, Iran. *Earth Sci Inf* 8(1):171–186
- Nampak H, Pradhan B, Abd Manap M (2014) Application of GIS based data driven evidential belief function model to predict groundwater potential zonation. *J Hydrol* 513:283–300
- Obi Reddy GP, Chandra MK, Srivastav SK, Srinivas CV, Maji AK (2000) Evaluation of groundwater potential zones using remote sensing data: a case study of Gaimukh watershed, Bhanadra District, Maharashtra. *J Indian Soc Remote Sens* 28:19–32
- Oh H, Kim Y, Choi J, Park E, Lee S (2011) GIS mapping of regional probabilistic groundwater potential in the area of Pohang City, Korea. *J Hydrol* 399:158–172
- Pareta K, Pareta U (2011) Hydromorphogeological study of Karawan watershed using GIS and remote sensing techniques. *E-Int Sci Res J* III(4):243–268
- Pothiraj P, Rajagopalan B (2013) A GIS and remote sensing based evaluation of groundwater potential zones in a hard rock terrain of Vaigai sub-basin, India. *Arab J Geosci* 6:2391–2407
- Pradeep R (1998) Remote sensing techniques to locate groundwater potential zones in upper Urmil River Basin, District Chhatarpur, central India. *J Indian Soc Remote Sens* 26(3):135–147
- Prasad RK, Mondal NC, Banerjee P, Nandakumar MV, Singh VS (2008) Deciphering potential groundwater zone in hard rock through the application of GIS. *Environ Geol* 55:467–475
- Rao PJ, Harikrishna P, Srivastav SK, Satyanarayana PVV, Rao BBD (2009) Selection of groundwater potential zones in and around Madhurwada Dome, Visakhapatnam District: a GIS approach. *J Indian Geophys Union* 13(4):191–200
- Ravindran KV, Jeyram A (1997) Ground water prospects of Shahbad Teshil, Baran District, eastern Rajasthan: a remote sensing approach. *J Indian Soc Remote Sens* 25(4):239–246
- Saha D, Dhar YR, Vittala SS (2010) Delineation of groundwater development potential zones in parts of marginal Ganga Alluvial Plain in South Bihar, eastern India. *Environ Monit Assess* 165:179–191
- Saraf AK, Choudhary ER (1998) Integrated remote sensing and GIS for ground water exploration and identification of artificial recharge sites. *Inter J Remote Sens* 19(10):1825–1841
- Sener E, Davraz A, Ozcelik M (2005) An integration of GIS and remote sensing in groundwater investigations: a case study in Burdur, Turkey. *Hydrogeol J* 13(5–6):826–834
- Shahid S, Nath SK, Roy J (2000) Groundwater potential modelling in a soft rock area using a GIS. *Int J Remote Sens* 21(9):1919–1924
- Sheffield C (1985) Selecting band combinations from multispectral data. *Photogrammetric Eng Remote Sens* 51(6):681–687
- Shendi EH (1989) New approach for locating promising water well sites in Saint Katherine and surroundings, South Sinai. In: *Proc. 2nd Conf. Geol. Sinai Develop., Suez Canal Univ., Ismailia, Egypt, 1989*, pp 97–102
- Shendi EH (1992) The role of El-Agramia plain in the development of Saint Catherine area, South Sinai. In: *Proc. 3rd Conf. Geol. Sinai Develop., Suez Canal Univ., Ismailia, Egypt, December 1992*, pp 55–62
- Shendi EH, Abou El-Magd A (2004) A new approach for ground geophysics in the development of groundwater in the basement terrains: a case study from Wadi Feiran, South Sinai, Egypt. *Proc. 7th Conf. Geol. Sinai Develop., Ismailia, Egypt, 2004*, pp 129–140
- Shendi EH, El-Rayes A (1992) Geophysical prospecting for groundwater in Wadi Sibaiya-Wadi El-Sheikh area, south Sinai. *M.E.R.C. Ain Shams Univ Earth Sci Ser* 6:55–61
- Sikdar PK, Chakraborty S, Adhya E, Paul PK (2004) Land use/land cover changes and groundwater potential zoning in and around Raniganj coal mining area, Bardhaman District, West Bengal: a GIS and remote sensing approach. *J Spatial Hydrol* 4(2):1–24
- Singh AK, Prakash SR (2003) An integrated approach of remote sensing, geophysics and GIS to evaluation of groundwater potentiality of Ojhala subwatershed Mirzapur district, UP, India. Presented at Map India Conference, New Delhi, 26–31 Jan. 2003
- Solomon S, Quiel F (2006) Groundwater study using remote sensing and geographic information systems (GIS) in the central highlands of Eritrea. *Hydrogeol J* 14:729–741
- Soulakellis N, Novak I, Zouros N, Lowman P, Yates J (2006) Fusing Landsat-5/TM imagery and shaded relief maps in tectonic and geomorphic mapping: Lesvos Island, Greece. *Photogrammet Eng Remote Sens* 6:693–700
- Srinivasa RY, Jugran KD (2003) Delineation of groundwater potential zones and zones of groundwater quality suitable for domestic purposes using remote sensing and GIS. *Hydro Sci J* 48:821–833

- Subba RN (2006) Groundwater potential index in a crystalline terrain using remote sensing data. *Environ Geol* 50(7):1067–1076
- Surabuddin MM, Pandey AC, Garg RD (2007) Groundwater prospects evaluation based on hydrogeomorphological mapping using high resolution satellite images: a case study in Uttarakhand. *J Indian Soc Remote Sens* 36:69–76
- Todd KD (1980) *Ground water hydrology*, 2nd edn. Wiley, New York
- Verstappen HT (1977) *Remote sensing in geomorphology*. Elsevier, New York
- Wachs D, Arad A, Olshina A (1979) Locating groundwater in the Santa Catherina area using geophysical methods. *Ground Water* 17(3): 258–263
- Youssef AM, Pradhan B, Hassan AM (2011) Flash flood risk estimation along the St. Katherine Road, southern Sinai, Egypt using GIS based morphometry and satellite imagery. *Environ Earth Sci* 62:611–623. doi:10.1007/s12665-010-0551-1